https://doi.org/10.5194/essd-2025-107
Preprint. Discussion started: 31 March 2025

Open Access Earth System Science Data Discussions

A high spatial resolution dataset of ecosystem services of 2000-2020 in China

Yue Liu[1,2], Wenwu Zhao[1,2], Zhijie Zhang[3], Jingyi Ding[1,2], Lixin Wang[4]

[1]Institute of Land Surface System and Sustainable Development, Faculty of Geographical Science, Beijing Normal University, Beijing 100875, China

[2]State Key Laboratory of Earth Surface Processes and Hazards Risk Governance (ESPHR) , Faculty of Geographical Science, Beijing Normal University, Beijing 100875, China

[3]Chinese Academy of Environmental Planning, Beijing 100012, China

[4]Department of Earth and Environmental Sciences, Indiana University Indianapolis, Indianapolis, IN, 46202, USA

Correspondence to: e-mail: Wenwu Zhao (zhaoww@bnu.edu.cn)

Abstract. Ecosystem services are the various benefits provided by ecosystems to humans, establishing a crucial link between the natural environment and human well-being. High-resolution ecosystem service datasets can provide more detailed and accurate information, enabling the identification of site-specific differences at local scales. In this study, we produced a high spatial resolution dataset of ecosystem services in China from 2000 to 2020, simulated using ecological process models. Model parameters were calibrated based on literature summaries, ground monitoring data, and reconstructed remote sensing data. The dataset, with a spatial resolution of 30 meters, includes net primary productivity, soil conservation, sandstorm prevention, and water yield. The validation results show high consistency between this ecosystem services dataset and both in situ observations and existing datasets. From 2000 to 2020, the overall trends for net primary productivity, soil conservation, and sandstorm prevention in China showed a weak increase, while water yield decreased during this period. This high-precision dataset provides a valuable scientific foundation for accurately assessing the provision of ecosystem services and supports evidence-based government decision-making. The dataset is made available at https://doi.org/10.57760/sciencedb.20797 (Liu et al., 2025) under a CC-BY 4.0 license.

1 Introduction

Ecosystem services are the benefits humans gain directly or indirectly from ecosystems (Costanza et al., 1997), serve as the foundation for human survival and development. Their supply is of great significance to ensure human well-being. According to the Millennium Ecosystem Assessment (MEA), ecosystem services can be categorized into provisioning services, regulating services, supporting services, and cultural services (MEA, 2005). At present, the resolution of most ecosystem service datasets is 250 meters or 1 km (Ouyang et al., 2016; Feng et al., 2012; IPBES, 2019). Although these

https://doi.org/10.5194/essd-2025-107
Preprint. Discussion started: 31 March 2025

datasets can provide valuable insights into large-scale ecosystem trends, studies on the localized impact of human activities, such as deforestation, urban expansion, agricultural intensification, and mining, require more detailed spatial and temporal information (Zhang et al., 2023; Hansen et al., 2013; Wu et al., 2024). This limitation also affects the ability to evaluate the effectiveness of measures such as protected area construction and ecological engineering implementation (Liu et al., 2023; Liu et al., 2024). Thus, high-resolution and long-term ecosystem service datasets are highly needed to support more effective ecosystem management and protection policies.

Accurate ecosystem service assessment relies heavily on high-quality data. However, detailed studies on ecosystem impacts caused by human activities remain constrained due to insufficient availability of high-resolution and long-term datasets. Land use is the foundation of ecosystem service assessment, and the land use changes directly impact the accuracy of these assessments (Costanza et al., 2014). Currently, due to data consistency issues, the land cover data used in ecosystem service assessment vary significantly. Examples include the European Space Agency Climate Change Initiative Land Cover Dataset (Peng et al., 2023), the Moderate Resolution Imaging Spectroradiometer (MODIS) Land Cover Dataset (Zhao et al., 2010), and the Landsat Dataset (Mugiraneza et al., 2019). However, these datasets still have limitations in terms of resolution and consistency. The GlobelLand 30 dataset is among the highest-resolution and most accurate global land use datasets available (Chen et al., 2015). It represents a significant resource for global land use research and applications. This dataset covers the world, ensuring data consistency and high accuracy, making it suitable for detailed ecosystem service assessments (Chen et al., 2015). Furthermore, most existing ecosystem service datasets lack sufficient temporal resolution to support long-term assessments. Addressing these challenges by developing ecosystem service datasets with both high spatial resolution and long temporal resolution based on the GlobeLand30 dataset would significantly enhance the precision and applicability of ecosystem service assessments. This will improve our understanding and management of human impacts on ecosystems, providing a robust scientific foundation for policy-making and environmental protection (Li et al., 2023; Chen et al., 2017).

The global ecosystem service dataset primarily comes from the Intergovernmental Science-Policy Platform on Biodiversity and Ecosystem Services (IPBES) global ecosystem service assessment (IPBES, 2019a). The IPBES assessments provide a comprehensive scientific basis for understanding the current state and changes in global ecosystem services (IPBES, 2019b). Although these data offer extensive coverage, their infrequent update poses significant challenges in meeting the demands of long-term research (Díaz-Reviriego et al., 2019). In China, the main sources of ecosystem service data are the studies conducted by Ouyang (2016). Their research provides a solid foundation for the quantitative evaluation of ecosystem services. However, most of their data focuses on the period around 2010 and lacks recent updates, limiting the comprehensive understanding of dynamic changes in ecosystem services. Similarly, contributions from Fang et al. (2018) are significant, but their datasets also suffer from discontinuity and infrequent updates (Fang et al., 2018). This inconsistency and lack of long-term updates severely limit the study of ecosystem services changes over time. Due to the lack of continuous data, it is currently challenging to accurately assess the combined impacts of land use and climate change on ecosystem services over recent decades (Xu et al., 2017). Long-term data are crucial

https://doi.org/10.5194/essd-2025-107
Preprint. Discussion started: 31 March 2025

for understanding the dynamic changes in ecosystem services, identifying driving factors, and formulating effective environmental protection policies (Wang et al., 2024; Wang et al., 2022). To address this issue, there is a need to develop high-resolution, long-term sequence ecosystem service datasets. This development will enhance the precision and applicability of ecosystem service assessments, helping scientists better understand and manage the impacts of human activities on ecosystems.

Verification of ecosystem service data is crucial for ensuring data quality, supporting scientific research, and informing policy-making (Jiang et al., 2021). The primary methods for validating ecosystem service data include cross-validation, error analysis, controlled experiments, and field observations. Cross-validation involves comparing results with different remote sensing data sources to ensure consistency (e.g., comparing the results with remote sensing data sets from different sources) (Feng et al., 2016). Error analysis assesses random errors and systematic errors (e.g., sensor calibration corrections) (Richardson et al., 2006; Zhang et al., 2023). Controlled experiments, both in the field and laboratory (e.g., measuring soil moisture under various management practices), ensure data accuracy and consistency (Bockheim et al., 2009). Additionally, comparing model predictions with measured data (e.g., carbon stock predictions from carbon cycle models versus field measurements) (Le Noë et al., 2023) and sensitivity analyses (e.g., assessing the impact of parameter changes on carbon stock predictions) further verify data accuracy and stability (Hooper et al., 2017). Current methods for data validation are constrained by several limitations, including insufficient field observations, heterogeneous data sources, and a lack of robust cross-validation methods. These shortcomings undermine the reliability and applicability of ecosystem service assessments, particularly in the context of complex and dynamic ecosystems. Consequently, the development of more accurate and comprehensive validation methods is crucial for improving the precision of ecosystem service dataset.

This study integrated various datasets such as remote sensing, *in situ* observations, and primary literature to obtain key parameters for ecosystem services. We used a series of models with clear mechanisms and data support from previous research. By incorporating and utilizing the GlobelLand 30 dataset, this study achieves higher-resolution assessments of ecosystem services in China, covering four key MEA-classified services: net primary productivity (NPP), classified as a supporting service, provides the foundation for biomass production and carbon cycling; soil conservation and sandstorm prevention, both regulating services, play a crucial role in mitigating land degradation, controlling erosion, and maintaining environmental stability; water yield, also a regulating service, is essential for sustaining hydrological cycles and ensuring water resource availability. This high-resolution dataset is valuable for assessing carbon sink capacity, mitigating global ecological risks such as land degradation and water scarcity, and providing scientific support for the implementation of ecological compensation mechanisms, land-use planning optimization, and the sustainable development of regional ecological economies (Ouyang et al., 2016). The aims of this work are (1) to construct the assessment models and datasets, (2) to map the ecosystem services in China, (3) to verify the ecosystem services data, and (4) to explore the ecosystem service dynamics.

https://doi.org/10.5194/essd-2025-107
Preprint. Discussion started: 31 March 2025

Open Access Earth System Science Data Discussions

2 Study area

The temporal and spatial patterns of China's ecosystem services are analyzed across 34 provincial administrative regions, including 23 provinces (Hebei, Shanxi, Liaoning, Jilin, Heilongjiang, Jiangsu, Zhejiang, Anhui, Fujian, Jiangxi, Shandong, Henan, Hubei, Hunan, Guangdong, Hainan, Sichuan, Guizhou, Yunnan, Shaanxi, Gansu, Qinghai, Taiwan), 5 autonomous regions (Inner Mongolia, Guangxi, Tibet, Ningxia, Xinjiang), 4 municipalities directly under the central government (Beijing, Tianjin, Shanghai, Chongqing), and 2 special administrative regions (Hong Kong, Macau), as shown in Fig. 1.

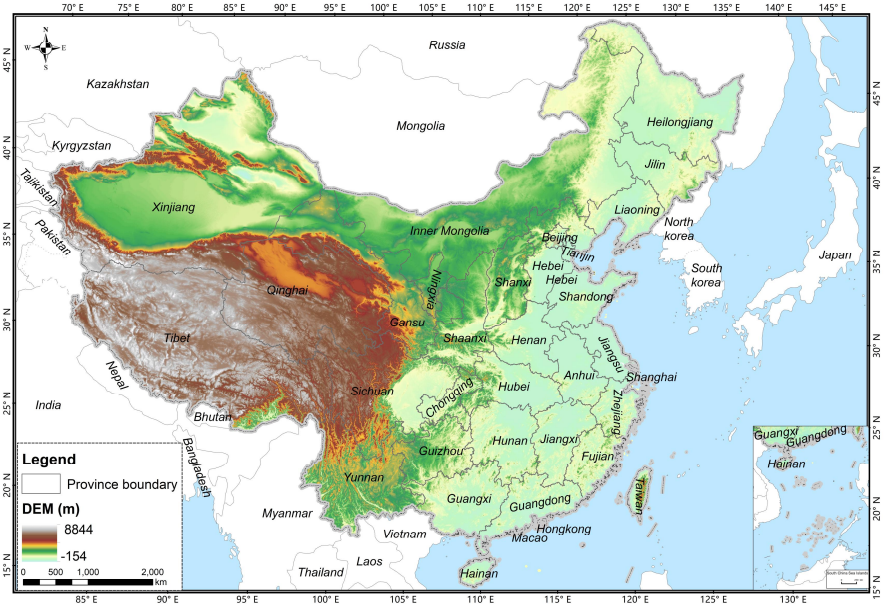

Figure 1: The study area.

3 Data and Methods

3.1 Ecosystem services assessment parameters and localization processing

This study uses the Carnegie-Ames-Stanford Approach (CASA) model, the Revised Universal Soil Loss Equation (RUSLE) model, the Revised Wind Erosion Equation (RWEQ) model, and the Integrated Valuation of Ecosystem Services and Tradeoffs (InVEST) model to assess the net primary productivity, soil conservation, sandstorm prevention, and water yield of China. The methods and datasets for assessing the four ecosystem services are shown in supplementary material (ecosystem service assessment methods) and Tab. S1. In this study, the datasets were projected to the Albers projection and resampled to a 30meters resolution to standardize the data.(Liu et al., 2023).

https://doi.org/10.5194/essd-2025-107
Preprint. Discussion started: 31 March 2025

3.1.1 Net primary productivity

Based on the nationally adapted CASA model (Zhu, 2005), this study calculated monthly net primary productivity (NPP) and summed these monthly values to obtain the annual NPP. Based on high-precision remote sensing data, this study localized the maximum and minimum values of NDVI and SR, as well as the maximum light use efficiency (ε_{max}) specific to various landcover types.

(1) Normalized Difference Vegetation Index (NDVI)

NDVI is an important parameter for estimating the absorbed photosynthetically active radiation (APAR) by vegetation (Jiao et al., 2021), and the accuracy of NPP mostly depends on the value of $NDVI_{i,min}$ and $NDVI_{i,max}$.

Following Zhu's method, GlobeLand 30 data were used as mask to extract the NDVI of each landcover using ArcGIS software. According to the pixel NDVI distribution probability, the corresponding DN values of NDVI 95% and 5% were selected as the $NDVI_{i,max}$ and $NDVI_{i,min}$, respectively (see the Tab. S2).

(2) Simple Ratio Vegetation Index (SR)

SR is a common vegetation index used to assess the amount of vegetation, and the details were shown in Eq. (6) in the supplementary materials. We extracted the SR values for each landcover type based on GlobeLand 30 data. According to the pixel SR distribution probability, the corresponding DN values of SR 95% and 5% were selected as the $SR_{i,max}$ and $SR_{i,min}$, respectively.

(3) Maximum light use efficiency (ε_{max})

The ε_{max} in this study was determined in three steps. First, this study calculated the APAR, temperature, and moisture stress for all pixels. Next, the measured NPP data were sourced from the National Ecosystem Research Network of China at the same period. Finally, the ε_{max} for each landcover were simulated based on the principle of minimizing error. For a certain landcover, the error between the measured and the simulated NPP can be expressed by the following formula:

$$E(x) = \sum_{i=1}^{j} (m_i - n_i x)^2 \quad x \in [l,u], \tag{1}$$

where i and j are the number of samples and the maximum number of samples of a certain landcover, respectively. m and n are the measured NPP and the product of APAR, temperature, and moisture stress, respectively. x is the simulated ε_{max} of a certain landcover. l and u are the maximum and minimum ε_{max} of landcover. Eq. (1) represents an upward-opening parabola, which guarantees the existence of a minimum value within the interval $[l, u]$. The corresponding x value at this minimum point represents the simulated ε_{max} for a certain landcover (see the Tab. S2).

3.1.2 Soil conservation

The Revised Universal Soil Loss Equation (RUSLE) model is widely used for large-scale soil conservation assessment at regional and global scales (Naipal et al., 2015) due to its simple structure and empirical basis. It mainly estimated the annual average soil conservation based on five factors, namely, rainfall erosivity factor (R factor), vegetation cover and management factor (C factor), soil erodibility factor (K factor), slope length factor (LS factor) and soil and water conservation measure factor (P factor) (Renard, 1997).

https://doi.org/10.5194/essd-2025-107
Preprint. Discussion started: 31 March 2025

(1) R factor

The R factor is mainly affected by continuous rain intensity. In this study, the R factor was calculated according to the empirical equation (see the Eq. (14) in the supplementary materials) of Wisohmeier and Smith (1978). The monthly precipitation data obtained from the National Earth System Science Data Center were resampled to 30 meters spatial resolution using ArcGIS software.

(2) C factor

The C factor represents how varying vegetation cover and management practices influence soil conservation (see the Eq. (19) in the supplementary materials). Vegetation coverage (Cov) was calculated using NDVI, and the calculation is expressed by the following formula:

$$Cov = \frac{(NDVI - NDVI_{min})}{(NDVI_{max} - NDVI_{min})} \times 100\%, \quad (2)$$

where $NDVI_{max}$ and $NDVI_{min}$ are the DN values of NDVI 95% and 5%, respectively.

(3) K factor

The K factor represents soil sensitivity to erosion from raindrop splash or surface runoff, influenced by rainfall, runoff, and infiltration. This study used the method developed by Williams et al. (1984) to estimate the K factor in the EPIC (erosion-productivity impact calculator) model (see Eq. (15) in the supplementary materials). The soil properties data used in this model was from International Soil Reference and Information Centre (ISRIC), and resampled to a 30 m spatial resolution.

(4) LS factor

The LS factor reflects the relationship between slope and terrain conditions and is essentially the distance over which raindrops or sediment flow until their energy is dissipated. The slope length factor (L factor) was calculated using the algorithm proposed by Delgado et al. (2024) (see Eq. (16) in the supplementary materials). the slope factor (S factor) was determined using different formulas depending on the slope range: for slopes below 10°, it was calculated using the formula proposed by McCool et al. (1987), and for slopes above 10°, the formula developed by Liu et al. (1994) was applied (see the Eq. (18) in the supplementary materials).

(5) P factor

The P factor is the ratio of soil loss after adopting specific measures to the soil loss when planting along the slope reflecting the differences in soil loss due to various vegetation management measures. Since field experiments were not conducted and remote sensing methods are challenging to apply nationwide, this study assigns P factor values based on landcover classifications, as derived from relevant literature (Tab. S3).

3.1.3 Sandstorm prevention

The the Revised Wind Erosion Equation (RWEQ) model includes five factors, namely soil erodibility factor (SEF), the soil crust factor (SCF), the vegetation factor (C), the soil roughness factor (K'), and the weather factor (WF).

(1) Soil erodibility factor (SEF)

The SEF factor reflects the soil's vulnerability to wind erosion under specific physical and chemical conditions. In this study, the SEF factor was calculated based on the relationship between soil physical and chemical properties and soil erodibility, as established by Fryrear et al. (1994). The formula can be

https://doi.org/10.5194/essd-2025-107
Preprint. Discussion started: 31 March 2025

found in Eq. (29) of the supplementary materials. The soil properties data used in this model come from ISRIC and resampled to a 30 m spatial resolutio.

(2) Soil crust factor (SCF)

The presence of soil crusts effectively reduces the content of erodible particles and diminishes the abrasive effect of airflow on soil particles (Zobeck et al., 2000). Hagen (1991) developed the equation for the SCF based on wind tunnel tests of soils with different physical and chemical properties (Eq. (30) in the supplementary materials). This study applies this equation to calculate the SCF. The source and processing method of soil properties data is the same as that of SEF.

(3) Vegetation factor (C)

C factor is essential for soil protection against wind erosion by covering the surface, increasing surface roughness, and aiding in the deposition of moving particles. The vegetation factor includes two parameters: vegetation cover (Cov) and the coefficient of different vegetation types. The calculation of Cov is provided in Eq. (2), while the coefficient is set based on related literature.

(4) Soil roughness factor (K')

K' factor indicates how terrain-induced surface roughness influences wind erosion and is primarily derived from DEM data processed in ArcGIS software (Eq. (31) in the supplementary materials).

(5) Weather factor (WF)

The WF factor represents the combined effect of various meteorological factors on wind erosion, with wind being the primary driving force. The WF factor is determined by three indicators: wind factor (Wf), soil moisture factor (SW), and snow cover factor (SD).

The Wf data were sourced from ECMWF Reanalysis v5 (ERA5), and relevant processing is completed on the GEE platform. SW was calculated from potential evapotranspiration and precipitation data. SD data were derived by aggregating 500 m observations from the 'MODIS/Terra Snow Cover Daily L3 Global 500 m Grid' dataset. All the datasets were resampled to a 30 m resolution using ArcGIS software.

3.1.4 Water yield

The water yield data of China (2000-2020) were obtained by merging the data from individual watersheds, and these watershed data were from the Ministry of Water Resources (China) (http://www.mwr.gov.cn/).

(1) Precipitation

The annual average precipitation data comes from the National Earth System Science Data Center (https://www.geodata.cn/) with 1000-meter (m) pixel resolution. These data were resampled to 30 meters and clipped into small watersheds according to the watershed vector.

(2) Potential evapotranspiration

The MOD16A2 dataset provides 8-day composite data on evapotranspiration/latent heat flux at 500-meter (m) pixel resolution. This study calculated the annual average potential evapotranspiration data, resampled them to 30 meters, and clipped them to obtain the potential evapotranspiration of the separate watersheds.

(3) Plant available water content (PAWC)

https://doi.org/10.5194/essd-2025-107
Preprint. Discussion started: 31 March 2025

PAWC represents the fraction of total soil water content that is accessible for plant growth. It is typically calculated using the following formula:

$$PAWC = FC - PWP, \quad (3)$$

where *FC* and *PWP* are the field capacity and permanent wilting point, respectively. The *FC* and *PWP* can be estimated based by soil properties, as detailed see the Eq. (40) in the supplementary materials. The soil properties data come from the SoilGrids dataset, which has a resolution of 250 meters. In this study, it has been resampled to 30 meters and clipped according to the watershed.

(4) Rooting depth

Rooting depth refers to the actual depth that the roots of various plants can reach across different landcover. In this study, we have obtained the rooting depth parameters in each landcover by combining findings from the literature and existing materials. The detailed information in see the Tab. S5 in the supplementary materials.

(5) Available water content (AWC)

AWC of the soil (mm) depends on soil properties and effective depth, determining its water storage and supply for plant growth. It is influenced by PAWC, as well as the maximum soil root depth and the plant's minimum root depth.

(6) Z value

The seasonal parameter Z is an empirical constant that reflects regional distribution of precipitation and hydrogeological factors. Donohue et al. (2012) through their study of Australia's climatic conditions that the seasonal parameter Z can be expressed as the following formula :

$$Z = 0.2 \times N, \quad (4)$$

where N represents the number of rainfall events per year. Based on the daily precipitation data of the National Meteorological Administration from 2000, 2010, and 2020, the average annual precipitation number of year was assigned a value N, and the seasonal parameters of the study area were calculated based on it.

(7) Evapotranspiration coefficient (Kc)

Kc is the evapotranspiration coefficient for each landcover type, and it estimates plant evapotranspiration for landcover.

$$K_c = \frac{\sum_{m=1}^{12} kc_m \times ET_{0m}}{\sum_{m=1}^{12} ET_{0m}}, \quad (5)$$

where kc_m is the average plant evapotranspiration coefficient in month m (January to December), and ET_{0m} is the potential evapotranspiration in month m. In this study, we utilized the methodology based on the vegetation evapotranspiration coefficients for different growth stages published by FAO-56 (Allen, 2000). Through a comprehensive literature review and analyzing of statistical yearbook data, this study identified the most widely distributed vegetation types across various landcover in China. Subsequently, the average evapotranspiration coefficients for these vegetation types over their whole life cycles were calculated. The evapotranspiration coefficient for each landcover was then represented by the mean of the coefficients of the different vegetation types within that category.

https://doi.org/10.5194/essd-2025-107
Preprint. Discussion started: 31 March 2025

3.2 Data processing

3.2.1 Landsat data

Landsat data provide more extended time series with a 30 m pixel resolution, with NDVI derived from Landsat 5 TM for 2000 and 2010, and Landsat 8 OLI for 2020. This study also adjusted the radiometric discrepancies between Landsat 5 and Landsat 8 sensors (Zhang et al., 2023) because their different spectral response functions (Markham and Helder, 2012).

NDVI was calculated in Google Earth Engine (GEE) using Landsat 5 and 8 Level 2, Collection 2, Tier 1 data, specifically utilizing the red, near-infrared, and quality evaluation (QA) bands. The time-series datasets were processed through three stages: (1) cloud masking, (2) reflectance calibration, (3) mosaic, reproject, and clip. Cloud, snow, and shadow pixels were identified the low-quality pixel and the image was masked using its QA layer. A scaling factor (Eq. (6)) was used to adjust the surface reflectance and surface temperature outputs before utilizing the data(Markham and Helder, 2012). To correct the surface reflectance data for Landsat 5 and 8, this study used the robust and verifiable correction approach (Eq. (7)) (Anderson et al., 2020). The Landsat 5 and 8 datasets were merged, and NDVI was calculated for each collected image (Eq. (8)). Finally, monthly and quarterly NDVI datasets were generated.

$$OpticalBands = 0.0000275 * SR\_B - 0.2, \tag{6}$$

$$TM = 0.0029 + 0.9589OLI, \tag{7}$$

$$NDVI = \frac{B_{NIR} - B_{RED}}{B_{NIR} + B_{RED}}, \tag{8}$$

where Optical Bands, SR_B, TM and OLI refer to the corrected bands, the visible spectrum bands, Landsat 5 data, and Landsat 8 data, respectively. B_{NIR} and B_{RED} represent the near-infrared band and red band of images, respectively.

Vegetation coverage was calculated through Eq. (2). NDVI and vegetation coverage mapping were were merged to cover China. The sinusoidal projection was transformed into the Albers projection, which is more suitable for large east-west oriented areas at mid-latitudes.

3.2.2 MODIS data

Evapotranspiration, potential evapotranspiration, and snow cover datasets used in this study were MODIS Level-2 products that adopt temporal registration, providing data with the same spatial resolution and covering the same geographic area.

This study identified and reconstructed the low-quality pixels of the MODIS images. Data reconstruction involves two main steps: filtering and restoration. Low-quality and missing pixels were identified as invalid and required reconstruction (Wan et al., 2014). This study used quality control labels from daily and monthly files as mask layers to detect low-quality pixels, ensuring the reliability of the remote sensing data. Monthly evapotranspiration data grid cells marked with “MODLAND_QC bits = 0 ”, and “ Cloud state = 0” in the ET_QC Bitmask layer are classified as high-quality data, with

https://doi.org/10.5194/essd-2025-107
Preprint. Discussion started: 31 March 2025

other pixels are considered low-quality pixels then set to missing values. This study initially identified invalid pixels in 8-day evapotranspiration images for each day of the month at the same locations, and then reconstructed these invalid daily pixels. The process of reconstructing invalid pixels involves three steps: (1) filling the invalid pixels with co-located in situ observations when available; (2) using geographically weighted regression (GWR) to interpolate invalid pixels when in situ data is absent, based on similar pixels from multiple sources; and (3) filling the remaining invalid pixels with data from the same month in adjacent years.

Then, these products were composited for eight days, so this study obtained monthly products by calculating the mean of the data for that month. Finally, the MODIS Reprojection Tool (MRT) was used to mosaic, reproject, and resampled the MODIS data to 30 meters to be consistent with the NDVI data.

3.2.3 Supplementary data

As one of the high-precision global land cover datasets, the overall accuracy of GlobeLand30 over 80.33%, which can provide detailed ground cover information (Chen et., 2015). Due to errors in the remote sensing sensors, slight offsets were observed in the 2020 data. This study used the ArcGIS software to correct the offset, mosaic, and reproject of the GlobeLand30 data.

Temperature, precipitation, soil properties, and digital elevation model data were mosaicked, reprojected, and resampled to 30 meters. Solar radiation and wind speed were obtained, reprojected, and resampled in GEE. *In situ* observation data was retrieved from the China Meteorological Administration (https://www.cma.gov.cn/).

4 Results

4.1 Validation

This study used simulated Net Primary Productivity (NPP) data and existing remote sensing datasets for cross-validation due to the lack of large-scale biomass monitoring data. Spawn et al. (2020) provided a global 300 m resolution map of aboveground and belowground biomass carbon density for 2010. This dataset was rigorously validated, and quality assessed by their original producers. This study randomly generated 2000 points on the map of China and extracted the values of the simulated NPP and Spawn's datasets in 2010. This study then performed a correlation analysis, with the results shown in Fig. 2(a). In addition, the NPP estimated in this study is multi-year monthly data, this study separately cross-validates the NPP for multiple years with remote sensing datasets (MODIS/Terra Net Primary Production Gap-Filled Yearly L4 (MOD17A3HGF), Resource and Environment Science and Data Center (RESDC), and Global Primary Production Data Initiative (GPPDI). Figure 3 presents t the validation of NPP data through comparisons with aboveground biomass datasets and three available NPP products.

Obtaining observed soil conservation data is generally challenging. Since soil conservation service is derived from soil erosion rates estimated by the RUSLE model, its reliability can be indirectly assessed by validating simulated soil erosion (Xiao et al., 2017). Therefore, this study used the watershed soil

https://doi.org/10.5194/essd-2025-107
Preprint. Discussion started: 31 March 2025

350 erosion data watershed soil erosion data to evaluate the model's accuracy (Liu et al., 2023). The watersheds include the Yangtze, Yellow, Huai, and Hai River Basins. This study obtained the soil erosion rates of these watersheds from 2000 to 2020 from the China Soil and Water Conservation Bulletin (http://www.mwr.gov.cn/sj/tjgb/zgstbcgb/) and simulated erosion rates were extracted using basin vectors provided by the Water Resources Department. Based on these two datasets, this study
355 performed a correlation analysis, with the results shown in Fig. 2 (b).

This study used simulated sandstorm prevention data and a remote sensing dataset for cross-validation due to the lack of monitoring data on sandstorm prevention. Gkikas et al. (2022) quantified the dust optical depth and characterized its monthly and interannual variability at both global and regional scales for the period 2003-2017, using a fine spatial resolution (0.1° x 0.1°). This study randomly
360 generated 50 points on the map of China and extracted the values of the simulated sandstorm prevention data and Gkikas' datasets in 2010. This study then performed a correlation analysis, with the results shown in Fig. 2(c).

Surface water resource data for each province were from the Water Resources Bulletin (http://www.mwr.gov.cn/sj/tjgb/szygb/) from 2000 to 2020, which are typically obtained through field
365 monitoring and statistical methods conducted by the water conservancy department. This study matched the water yield simulated by the InVEST model with the actual water yield data from the bulletin. To ensure consistency, this study aligned the data based on the same provinces and the same years. Due to missing data for some provinces in the year 2000, this study matched the data for 2010 and 2020 for analysis. This study performed a correlation analysis on the matched datasets. The
370 Pearson correlation coefficient between the actual water yield and the simulated water yield was calculated to assess the consistency between the two datasets. The results are shown in Fig. 2(d).

https://doi.org/10.5194/essd-2025-107
Preprint. Discussion started: 31 March 2025

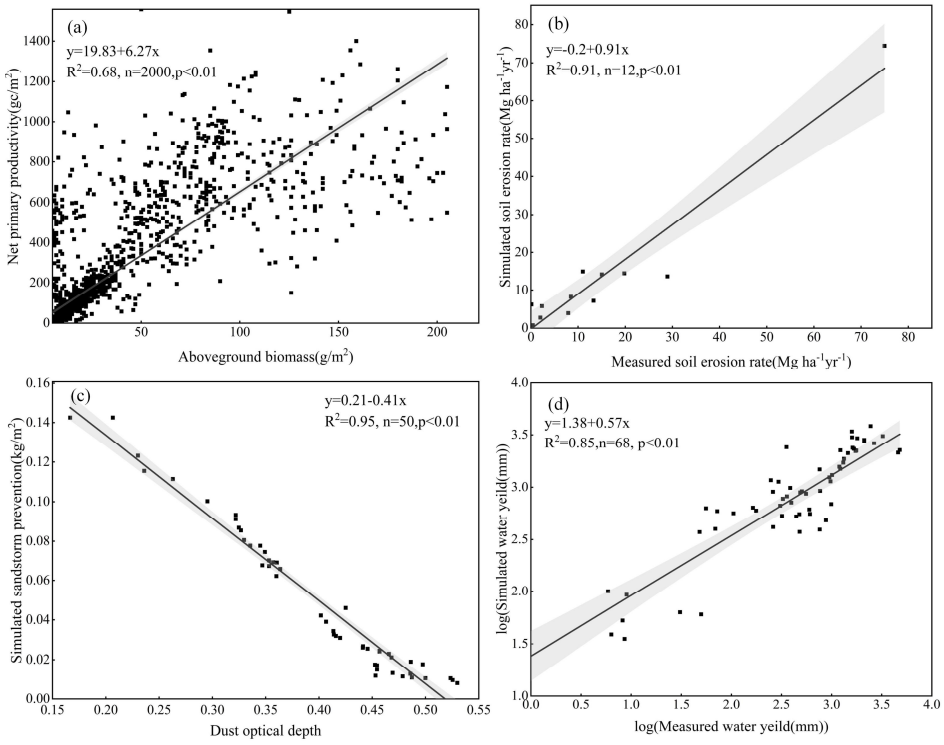

Figure 2: Validation of the assessment model in this study, (a) the aboveground biomass and NPP of China in 2010, (b) the simulations and measurement of annual soil erosion rates for six river basins, including those of the Yangtze, Yellow, Haihe, Huaihe, Pearl, and Songhua and Liaohe in 2000 and 2010, (c) the simulated sandstorm prevention and dust optical depth of China in 2010, (d) the simulations and measurement of water yield for 34 provinces in 2000 and 2020.

https://doi.org/10.5194/essd-2025-107
Preprint. Discussion started: 31 March 2025

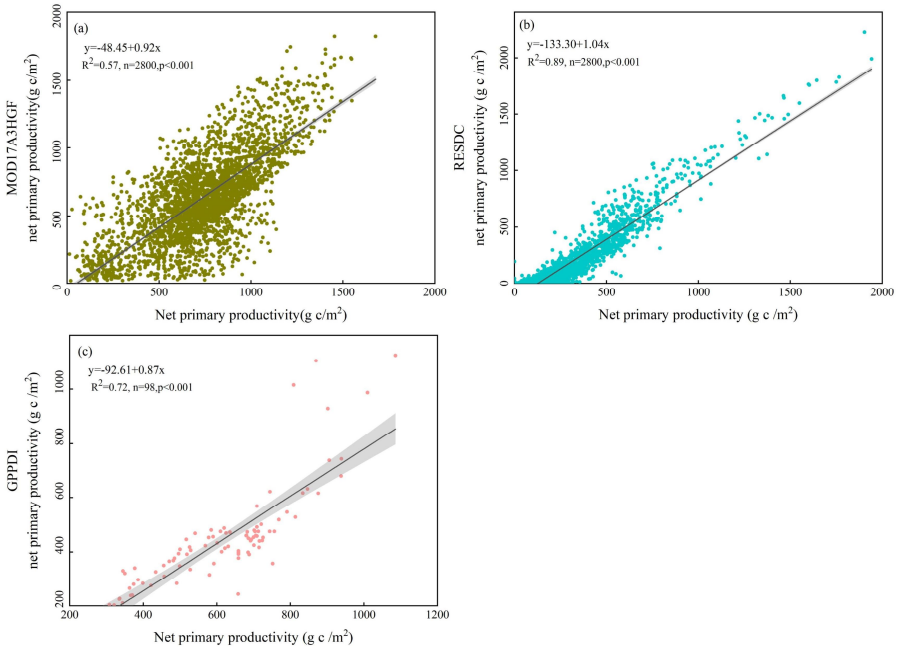

Figure 3: Validation of the NPP in this study, (a) the NPP estimated in this study and MODIS/Terra Net Primary Production Gap-Filled Yearly L4 (MOD17A3HGF), (b) the NPP estimated in this study and Resource and Environment Science and Data Center (RESDC) NPP data, (c) the NPP estimated in this study and Global Primary Production Data Initiative (GPPDI) NPP data.

4.2 Net primary productivity dynamics

The spatial distribution of net primary productivity (NPP) showed significant regional differences, generally showing an increasing trend along the rainfall-temperature gradient from northwest to southeast (Fig. 4). In 2020, high NPP regions were mainly distributed in Yunnan, Sichuan, Guangdong, Guangxi, and Heilongjiang, accounting for 9%, 9.27%, 3.80%, 4.86%, and 5.97% of China, respectively (Tab. S6). The total NPP increased by 0.45 Pg over the 20 years, with an increase of 11.31% (Fig. S2). The NPP of Yunnan, Inner Mongolia, Sichuan, Shanxi, Hebei, and Shaanxi increased, accounting for 28.04%, 8.69%, 20.82%, 15.89%, 14.44%, and 13.54% of the NPP dynamics from 2000 to 2020, respectively (Tab. S7).

These results are similar to those of Ouyang et al. (2016) who also found significant regional differences in NPP across different areas of China, with an overall increasing trend. This finding is consistent with other studies, such as Feng et al. (2016), which indicated that NPP significantly increased in the Loess Plateau region through vegetation restoration measures. This trend is further corroborated by Zhao et al. (2019), who observed that NPP in China's ecosystems has increased in recent decades, especially in the southeastern regions with relatively high precipitation and temperature.

https://doi.org/10.5194/essd-2025-107
Preprint. Discussion started: 31 March 2025

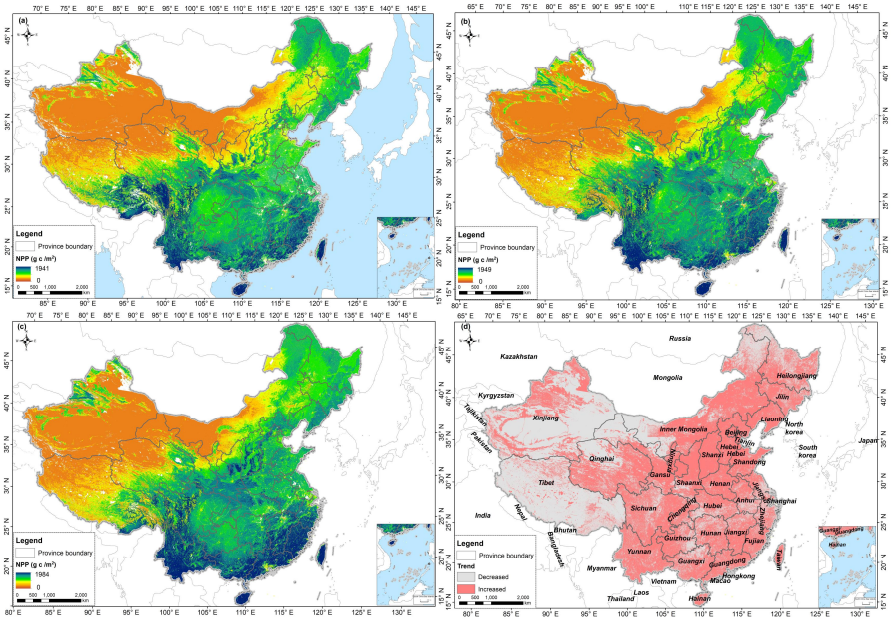

Figure 4: Spatial and temporal distribution of net primary productivity (NPP) in China from 2000 to 2020. (a) 2000 NPP; (b) 2010 NPP; (c) 2020 NPP; (d) NPP dynamics from 2000 to 2020.

4.3 Soil conservation dynamics

Soil conservation is primarily concentrated in the Sichuan Basin, Loess Plateau, and surrounding mountainous and hilly areas, eastern Great Khingan, and the Yunnan-Guizhou Plateau (Fig. 5). In 2020, the province with the most soil conservation quantity is Tibet (24.35%), while the least is Macao (0.00001%) (Tab. S6). Over the 20 years, total soil conservation increased by 184 million tons, with an increase rate of 13.67% (Fig. S2). The regions where soil conservation increased over the 20 years were Yunnan, Sichuan, Gansu, and Tibet, with reductions of 50, 19, 27, and 42 million tons, respectively (Tab. S7), accounting for 19.74%, 7.502%, 10.66%, and 16.58% of the soil conservation dynamics from 2000 to 2020 (Tab. S7). The decrease in soil conservation is mainly in the three provinces (regions) of Jilin, Hainan, and Guizhou, with increases of 20, 7, and 3 million tons, respectively, accounting for 0.79%, 2.76%, and 1.18% of the dynamic soil conservation from 2000 to 2020 (Tab. S7).

The results of this study are consistent with Ouyang et al. (2016) who found that implementing ecological restoration measures and vegetation reconstruction effectively controlled soil erosion in regions such as the Loess Plateau, resulting in high soil conservation values. Additionally, other studies have shown that through vegetation restoration measures and proper land management, the soil conservation capacity in most regions of China has significantly improved (Li et al., 2023).

https://doi.org/10.5194/essd-2025-107
Preprint. Discussion started: 31 March 2025

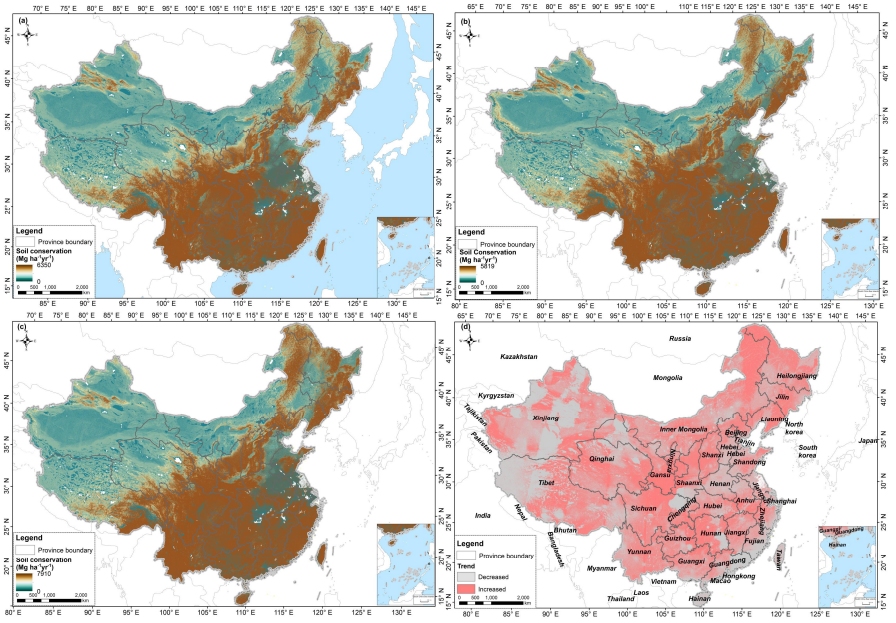

Figure 5: Spatial and temporal distribution of soil conservation in China from 2000 to 2020. (a) 2000 soil conservation; (b) 2010 soil conservation; (c) 2020 soil conservation; (d) Soil conservation dynamics from 2000 to 2020.

4.4 Sandstorm prevention dynamics

Sandstorm prevention is mainly distributed in arid and semi-arid areas of China, with significant quantities found in the western Alxa Plateau, Hexi Corridor, Junggar Basin, Tarim Basin, and eastern Qaidam Basin (Fig. 6). Over the 20 years, the sandstorm prevention increased by 18.67 million tons, with an increased rate of 78.94% (Fig. S2). During this period, the sandstorm prevention showed an increasing trend. The provinces (regions) where sandstorm prevention increased include Inner Mongolia, Ningxia, Xinjiang, Gansu, Tibet, Shaanxi, and Qinghai, with increases of 1095.04, 110.46, 287.05, 211.69, 28.89, 73.02, and 60.96 million tons, respectively, accounting for 58.65%, 5.92%, 15.37%, 11.34%, 1.55%, 3.91%, and 3.26% of the sandstorm prevention dynamics from 2000 to 2020 (Tab. S7).

The results of this study align with Xu et al. (2017), who observed that sandstorm prevention efforts are predominantly focused in the Northwestern region, including Mongolia's Ordos Plateau and Hunshandake. Some studies have also found that through vegetation restoration projects and ecosystem management measures, significant success has been achieved in sandstorm prevention in China. These measures have not only effectively reduced the frequency and intensity of sandstorms but also promoted the restoration and health of ecosystems. For instance, Ouyang et al. (2016) demonstrated that ecological restoration projects significantly improve soil retention and reduce sandstorms. Similarly, the study by Feng et al. (2016) supports these findings, emphasizing the crucial role of vegetation restoration in the Loess Plateau.

https://doi.org/10.5194/essd-2025-107
Preprint. Discussion started: 31 March 2025

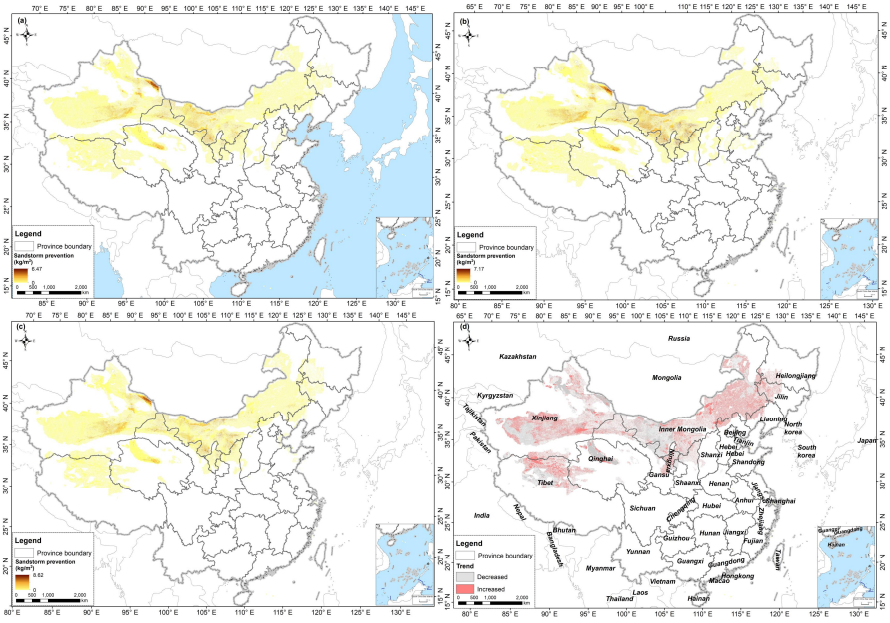

445 **Figure 6: Spatial and temporal distribution of sandstorm prevention in China from 2000 to 2020. (a) 2000 sandstorm prevention; (b) 2010 sandstorm prevention; (c) 2020 sandstorm prevention; (d) Sandstorm prevention dynamics from 2000 to 2020.**

4.5 Water yield dynamics

The water yield sis higher in the southeast and lower in the northwest, and gradually decreasing from
450 east to west (Fig. 7). The provinces that have high water yields are Yunnan, Sichuan, Guangdong, Guangxi, Jiangxi, Hunan, Hubei, and Heilongjiang, accounting for 6.90%, 7.37%, 5.56%, 6.65%, 5.46%, 5.19%, 6.51%, and 5.28% of the total national water production (Tab. S6). Over the 20 years, the water yield decreased by 60.64 mm/m^2, with a reduction rate of 13.53% (Fig. S2). The regions where water yield decreased are Yunnan, Guangdong, Guangxi, and Fujian provinces, with reductions
455 of 9.33, 5.85, 6.03, and 2.06 mm/m^2, respectively, accounting for 15.42%, 9.67%, 9.96%, and 3.405% of the dynamic water yield from 2000 to 2020. The increased province (regions) are Inner Mongolia, Sichuan, Anhui, and Hubei provinces, with increases of 9.82, 4.77, 7.37, and 11.24 mm/m^2, respectively, accounting for 16.23%, 7.88%, 12.18%, and 18.58% of the dynamic water yield from 2000 to 2020 (Tab. S7).

460 The results are in agreement with those of Yin et al. (2020), who identified a trend of higher water yield in the southeast and lower water yield in the northwest of China. High values are concentrated in the Sichuan-Yunnan-Loess Plateau ecological barrier and the southern mountainous areas, while lower values are found in the northwestern Qinghai-Tibet Plateau ecological barrier and the northern sand control zone. The water yield shows a declining trend, with reductions mainly in the southeastern
465 Sichuan-Yunnan-Loess Plateau and the central-southern mountainous areas.

https://doi.org/10.5194/essd-2025-107
Preprint. Discussion started: 31 March 2025

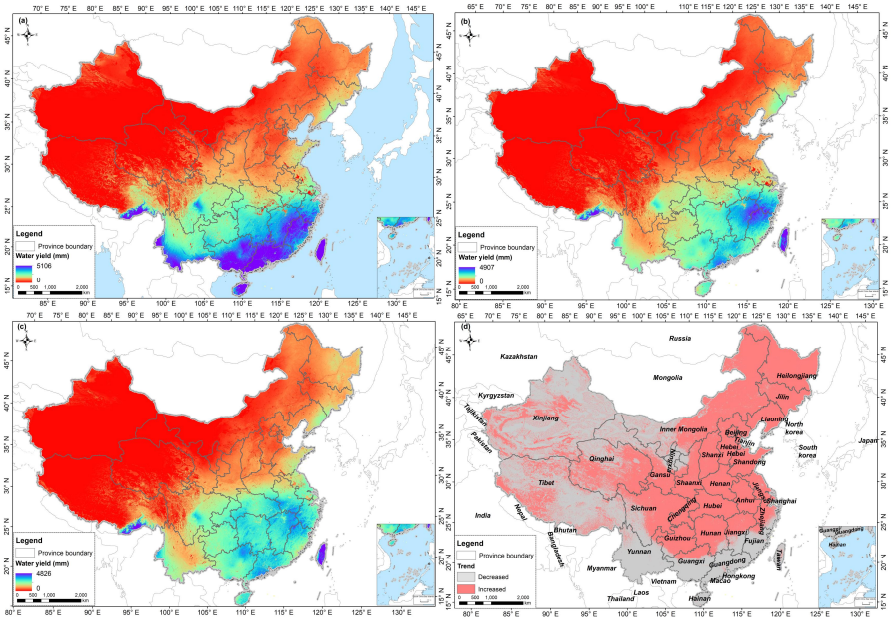

Figure 7: Spatial and temporal distribution of water yield in China from 2000 to 2020. (a) 2000 water yield; (b) 2010 water yield; (c) 2020 water yield; (d) Water yield dynamics from 2000 to 2020.

5 Discussion

5.1 Ecosystem services dynamics

The provincial differences in ecosystem services are mainly affected by area, terrain, climate, and land cover. Yunnan, Sichuan, Guangdong, Guangxi, and Heilongjiang have good hydrothermal conditions and vegetation growth. Ecological initiatives like the Natural Forest Protection Project and Shelterbelt Project in the Upper-middle Reaches of the Yangtze River, have positively impacted net primary productivity (NPP). Meanwhile, negative human activities such as deforestation have relatively low interference, resulting in higher net primary productivity in these regions (Lu et al., 2018). Sichuan, Xinjiang, Tibet, and Qinghai have more soil retention, due to the large administrative area of these provinces. These provinces have rugged terrain and most of the land cover is barren, which easily leads to soil erosion (Rao et al., 2023). Inner Mongolia, Xinjiang, Gansu, and Qinghai belong to arid or semi-arid climates, with relatively low precipitation and dry soil, making them prone to wind erosion and sandstorms due to high wind speeds and extensive barren (Piao et al., 2020). Yunnan, Sichuan, Guangdong, Guangxi, Jiangxi, Hunan, Hubei, and Heilongjiang have greater water yield due to

https://doi.org/10.5194/essd-2025-107
Preprint. Discussion started: 31 March 2025

abundant rainfall, complex terrain with various landforms such as mountains, plateaus, and hills, which facilitates the formation and accumulation of precipitation. Moreover, these regions are mostly covered by rich vegetation, and the transpiration effect of vegetation promotes precipitation formation and circulation (Yang et al., 2023).

In recent decades, China has implemented ambitious ecological projects, such as the Natural Forest Protection Project (NFPP), the Grain for Green Program (GFGP), the Three-north Shelter Forest Project (TSFP) and the Project for Preventing and Controlling Desertification (PPCD). The implementation of these projects has changed the land cover and effectively increased the vegetation coverage and improved stability of ecosystems (Cai et al., 2022). Concurrently, warming temperatures in recent years have also supported the vegetation growth (Song et al., 2021), contributing to a general increase in net primary productivity (NPP). The enhanced NPP reflects improved photosynthetic capacity driven by vegetation recovery, particularly in areas targeted by national restoration projects. The expansion of forests, shrubs, and grasslands under these ecological programs has strengthened vegetation and root systems, improving soil stability and sand retention capacity. This improvements have led to notable increases in soil conservation, particularly within watersheds affected by reforestation and revegetation efforts (Wang et al., 2016). The spatial patterns of increased soil conservation closely with the implementation areas of the GFGP and NFPP. Simultaneously, the observed reduction in desertified land and improvements in sandstorm prevention capacity correspond well with the effects of the TSFP and anti-desertification efforts (Li et al., 2023). These spatial patterns indicate that this high-resolution dataset can serve as an effective tool for assessing the ecological outcomes of national policy initiatives. Nevertheless, the increased vegetation cover has also affected hydrological processes, particularly through increased evapotranspiration and reduced surface runoff, which may result in declining water yield in afforested regions (Zhao et al., 2021). This highlights the importance of considering potential trade-offs between restoration benefits and water resource availability, especially in arid and semi-arid regions.

By revealing the relationship between changes in ecosystem service and policy measures, this dataset provides a scientific basis for multi-level governments and ecological management agencies to achieve sustainable landscape governance.

https://doi.org/10.5194/essd-2025-107
Preprint. Discussion started: 31 March 2025

5.2 Data accuracy and validation

In the previous studies, the resolution of land use data commonly used in ecosystem service assessment is mainly concentrated at 300 meters, 500 meters, or even 1000 meters (Peng et al., 2023; Zhao et al., 2010; IPBES, 2019). These data provide a holistic perspective for large-area analysis but are insufficient in terms of details (Li et al., 2023). For example, at a resolution of 300 meters, the accuracy of the identification and boundaries of land feature types is limited, which leads to the lack of detailed descriptions and accurate spatial distribution information in areas with complex terrain and diverse land use types (Yang et al., 2017). In contrast, this study used a dataset with a resolution of 30 meters, which enabled us to capture more detailed geographic features and land use changes during the assessment process, thereby providing richer and more detailed assessment results (Chen et al., 2015). The 30-meter resolution data allows us to more accurately identify and quantify different land feature types, such as buildings, farmland, forests, wetlands, etc., and to more accurately delineate their spatial distribution and boundaries (Kuang et al., 2021). Compared with the low resolution, this dataset shows significant advantages in land use classification accuracy and the completeness of spatial information. This refined data resolution helps to better understand and manage the provision of ecological services in complex ecosystems and also provides more targeted and operational data support for regional planning and environmental management decisions.

To ensure the reliability and accuracy of the data, this study used cross-validation, field observations, and statistical data to verify the accuracy and credibility of the 30-meter resolution ecosystem service dataset in terms of spatial distribution and quantity estimation. After detailed verification and analysis, this dataset showed higher accuracy and reliability (Fig. 3, Fig. 4). These verification work verified the application potentials of the dataset in ecosystem service assessment and provided a reliable data basis for subsequent related research and practical applications. In addition, this dataset has been used in studies such as exploring the effectiveness evaluation of protected areas (Liu et al., 2023) and the impact of urban urbanization on the dynamics of urban vegetation in China (Zhang et al., 2023). Through the dual verification of verification and application, this dataset has been fully verified and tested in practice, showing its reliability and practicality in various complex environments and application scenarios.

https://doi.org/10.5194/essd-2025-107
Preprint. Discussion started: 31 March 2025

5.3 Limitations and Uncertainties

This study used the remote sensing datasets and meteorological station data to construct long-term series NDVI, vegetation coverage, evapotranspiration, potential evapotranspiration, and snow cover datasets in China. These datasets effectively removed the missing or low-quality pixels in the original images, overcame the challenge of reconstructing data under cloud cover with limited information, and improved the precision of the monthly data.. Although we used high-precision data to assess ecosystem services, there are several uncertainties and limitations. For example, we calibrated the Landsat 5 and 8 spectral response data and calculated monthly and quarterly NDVI. However, there remains the possibility that sensor-related bias has not been fully eliminated (Anderson et al., 2020). Also, although this study extensively utilize site data to maximize the information available, enhancing the spatial and temporal continuity, the ground observation data still face representativeness issues, and the accuracy requires improvement in certain areas. Validating remote sensing products with site observation data is also subject to representativeness challenges, and uncertainties still exist in the accuracy verification process (Zhao et al., 2020). Finally, we assessed ecosystem services using different satellite sources data, which still affects the accuracy of ecosystem services even if they are resampled to the same spatial resolution (Liu et al., 2023).

Model-based assessments of ecosystem services inevitably involve multiple sources of uncertainty. These uncertainties primarily arise from errors in input data (such as climate variables, land cover types, and soil parameters, etc.) which propagate through the modeling process and have a cumulative effect on the results (Walther et al., 2025). Although cross-validation with existing products and ground-based observations demonstrates the overall robustness of dataset, this study did not conduct a systematic approach to quantifying uncertainty. Future studies should incorporate quantitative uncertainty analysis, such as sensitivity analysis and error propagation analysis, to provide confidence intervals for key ecosystem service estimates. These potential uncertainties should be carefully considered when applying this dataset to fine-scale ecological planning, ecosystem restoration decision-making, and the design of payment for ecosystem services (PES) schemes.

5.4 Application potentials

This dataset is widely applicable to various research and application scenarios, particularly in domains requiring high-resolution analysis such as urbanization monitoring, nature reserve management, and

https://doi.org/10.5194/essd-2025-107
Preprint. Discussion started: 31 March 2025

policy implementation assessment. It also provides robust data support for long-term ecosystem change research. The potential users of this dataset include government decision-makers, land-use planning and management agencies, environmental protection and natural resource management institutions, and researchers. Government policymakers can use this dataset to quantitatively assess the effectiveness of ecological restoration policies (e.g., the Grain for Green Programs and the Natural Forest Protection program), optimize land-use planning, and establish payment for ecosystem services (PES) schemes. Land-use planning and management agencies can leverage this dataset for urban expansion monitoring and land-use optimization, contributing to the development of sustainable strategies. Environmental protection organizations can utilize this dataset to monitor biodiversity, habitat changes, and ecosystem functions within nature reserves, providing scientific support for conservation and restoration efforts. Researchers can employ this dataset as a high-precision foundation for studies on ecosystem services, climate change, and land-use change, improving the accuracy and reliability of model-based analyses. Furthermore, this dataset demonstrates exceptional performance in long-term dynamic change analysis, accurately capturing and analyzing trends in ecosystem services across different regions, thus offering critical data support and an decision-making foundation for ecosystem management, environmental protection, and sustainable development.

6 Data availability

This dataset is essential for various geoscience research, particularity in understanding ecosystem responses to climate change, water resource management, environmental protection, and management. The dataset is openly available at https://doi.org/10.57760/sciencedb.20797 (Liu et al., 2025). All data are produced and generated in the ArcGIS, with the format being TIFF. They can be viewed and utilized in visualization geographic information systems or remote sensing industry software that supports the aforementioned format.

7 Conclusion

Mapping high-resolution ecosystem services is essential for understanding and managing China's ecosystems, particularly in achieving carbon neutrality and sustainable development goals. Existing ecosystem service datasets are often limited by low spatial resolution, outdated datasets, and data

https://doi.org/10.5194/essd-2025-107
Preprint. Discussion started: 31 March 2025

inconsistencies, which constrain their applicability at regional and local scales. In this study, we integrated the high precision remote sensing data and ground observations to produce high-resolution maps of four key ecosystem services in China, including one provisioning services - net primary productivity, and three regulating services - soil conservation, sandstorm prevention, and water yield. The mapping process employed robust ecological process models and achieved a dataset with 30-meter spatial resolution. Through comparison and cross-validation with other data sources, this dataset has been proven to have significant advantages in accuracy and applicability. This dataset has the advantages of high spatial resolution and long time series, and is expected to provide data support for the implementation effect evaluation of major ecological restoration programs such as Grain for Green Program and the Natural Forest Protection Program. In addition, this dataset can also be used to guide land use optimization, ecological restoration strategy formulation, and the design and implementation of incentive mechanisms based on ecosystem services (such as ecological compensation system).

Acknowledgments

This work was supported by the Third Xinjiang Scientific Expedition Program (No.2022xjkk0405), the 111 project, and the Fundamental Research Funds for the Central Universities of China.

Author contributions

Y L & Z J Z: Methodology, Software, Visualization, Writing - original draft preparation; W W Z & J Y D: Conceptualization, Formal analysis, Writing - review & editing, Supervision; L X W: Writing - review & editing.

Competing interests

The contact author has declared that none of the authors has any competing interests.

https://doi.org/10.5194/essd-2025-107
Preprint. Discussion started: 31 March 2025

References

Allen, R.G.: Using the FAO-56 dual crop coefficient method over an irrigated region as part of an evapotranspiration intercomparison study, J. Hydrol., 299 (1), 27-41, https://doi.org/10.1016/S0022-1694(99)00194-8, 2000.

Anderson, K., Fawcett, D., Cugulliere, A., Benford, S. ,Jones, D., Leng, R.L.: Leng Vegetation expansion in the subnival Hindu Kush Himalaya, Glob. Chang, Biol., 26, 1608-1625, https://doi.org/10.1111/gcb.14919, 2020.

Bockheim, J.G., Gennadiyev, A.N.: The value of controlled experiments in studying soil-forming processes: A review, Geoderma., 152(3-4), 208-217, https://doi.org/10.1016/j.geoderma.2009.06.019, 2009.

Budyko, M.I.: Climate and life, Academic Press, New York, USA, ISBN 0-12-139450-4, 1974.

Bush, A., Sollmann, R., Wilting, A., Bohmann, K., Cole, B., Balzter, H., Martius, C., Zlinszky, A., Calvignac-Spencer, S., Cobbold, A., Dawson, T., Emerson, B., Ferrier, S., Gilbert, M., Herold, M., Jones, L., Leendertz, F.H., Matthews, L., Millington, J.D.A., Olson, J.R., Ovaskainen, O., Raffaelli, D., Reeve, R., Rödel, M., Rodgers, T.W., Snape, S., Visseren-Hamakers, I., Vogler, A.P., White, P.C.L., Wooster, M.J., Yu, D.W.: Connecting Earth observation to high-throughput biodiversity data, Nat Ecol Evol., 1, 0176, https://doi.org/10.1038/s41559-017-0176, 2017.

Cai, Y., Zhang, F., Duan, P.: Vegetation cover changes in China induced by ecological restoration-protection projects and land-use changes from 2000 to 2020, Catena., 217, 106530, https://doi.org/10.1016/j.catena.2022.106530, 2022.

Cavender-Bares, J., Schneider, F.D., Santos, M.J., Armstrong, A., Carnaval, A., Dahlin, K.M., Fatoyinbo, L., Hurtt, G.C., Schimel, D., Townsend, P.A., Ustin, S.L., Wang Z., Wilson, A.M.: Integrating remote sensing with ecology and evolution to advance biodiversity conservation, Nat Ecol Evol., 6, 506–519, https://doi.org/10.1038/s41559-022-01702-5, 2022.

Chen, W., Liu, W., Geng, Y., Brown, M.T., Gao,C., Wu, R.: Recent progress on energy research: a bibliometric analysis, Renew. Sust. Energ. Rev., 73, 1051-1060, https://doi.org/10.1016/j.rser.2017.02.041, 2017.

Chen, J., Chen, A., Liao, X., Cao, L. ,Chen, X., He, C., Han, G., Peng, S., Lu, M., Zhang, W., Tong, X., Mills, J.: Global Land Cover Mapping at 30m Resolution: A POK-based Operational Approach. ISPRS J. Photogramm. Remote Sens., 103 (5), 7-27, https://doi.org/10.1016/j.isprsjprs.2014.09.002, 2015.

Chen, J., Cao, X., Peng, S., Ren, H.: Analysis and Applications of GlobeLand30: A Review. ISPRS Int. J. Geo-Inf., 6(8), 230, https://doi.org/10.3390/ijgi6080230, 2017.

Costanza, R., d'Arge, R., de Groot, R., Farber, S., Grasso, M., Hannon, B, Limburg, K., Naeem, S., O'Neill, R.V., Paruelo, J., Raskin, R.G., Sutton,P., van den Belt, M.: The value of the world's ecosystem services and natural capital, Nature., 387(6630), 253-260, https://doi.org/10.1038/387253a0, 1997.

Costanza, R., de Groot, R., Braat, L. Kubiszewski, I., Fioramonti, L., Sutton, P., Farber, S., Grasso, M.: Twenty years of ecosystem services： How far have we come and how far do we still need to go? Ecosyst. Serv., 28, 1-16, https://doi.org/10.1016/j.ecoser.2017.09.008, 2017.

Costanza, R., Groot, R., Sutton, P., van der Ploeg, S., Anderson, S.J., Kubiszewski, I., Farber,S., Turner, R.K.: Changes in the global value of ecosystem services, Global Environ. Change., 26, 152-158, https://doi.org/10.1016/j.gloenvcha.2014.04.002, 2014.

https://doi.org/10.5194/essd-2025-107
Preprint. Discussion started: 31 March 2025

Daily, G.C., Ruckelshaus, M.: 25 years of valuing ecosystems in decision-making, Nature., 606 (7914), 465-466, https://doi.org/10.1038/d41586-022-01480-x, 2022.

Dang, A.N., Jackson, B.M., Benavidez, R., Tomscha, S.A.: Review of ecosystem service assessments: Pathways for policy integration in Southeast Asia, Ecosyst. Serv., 49, 101266, https://doi.org/10.1016/j.ecoser.2021.101266, 2021.

Delgado, D., Sadaoui, M., Ludwig, W., Méndez, W.: DEM spatial resolution sensitivity in the calculation of the RUSLE LS-Factor and its implications in the estimation of soil erosion rates in Ecuadorian basins. Environ Earth Sci., 83, 36, https://doi.org/10.1007/s12665-023-11318-y, 2024.

Díaz-Reviriego, I., Turnhout, E. Beck, S.: Participation and inclusiveness in the Intergovernmental Science-Policy Platform on Biodiversity and Ecosystem Services, Nat Sustain., 2, 457-464, https://doi.org/10.1038/s41893-019-0290-6, 2019.

Donohue, R.J., Roderick, M.L., Mcvicar, T.R.: Roots, storms and soil pores: Incorporating key ecohydrological processes into Budyko's hydrological model, J. Hydrol., 436-437, 35-50, https://doi.org/10.1016/j.jhydrol.2012.02.033, 2012.

Fang, J., Yu, G., Liu, L., Hu, S., Chapin, F. S.: Climate change, human impacts, and carbon sequestration in China, Proc. Natl. Acad. Sci. U.S.A., 115(16), 4015-4020, https://doi.org/10.1073/pnas.1700304115, 2018.

Feng, X., Fu, B., Piao, S.Wang, S., Ciais, P., Zeng, Z., Lü, Y., Zeng, Y., Li, Y., Jiang X., Wu B.: Revegetation in China's Loess Plateau is approaching sustainable water resource limits, Nature Clim Change., 6, 1019-1022, https://doi.org/10.1038/nclimate3092, 2016.

Feng, X.M., Sun, G., Fu, B.J., Su, C.H., Liu, Y., Lamparski, H.: Regional effects of vegetation restoration on water yield across the Loess Plateau, China. Hydrol. Earth Syst. Sci., 16(8), 2617-2628, https://doi.org/10.5194/hess-16-2617-2012, 2012.

Fryrear, D.W., Krammes, C.A., Williamson, D.L., Zobeck, T.M.: Computing the wind erodible fraction of soils, J Soil Water Conserv., 49(2), 183-188, https://www.proquest.com/scholarly-journals/computing-wind-erodible-fraction-soils/docview/220961018/se-2, 1994.

Fu, Q., Li, B., Hou, Y., Bi, X., Zhang, X.: Effects of land use and climate change on ecosystem services in central Asia's arid regions: a case study in altay prefecture, China, Sci Total Environ., 607, 633-646, https://doi.org/10.1016/j.scitotenv.2017.06.241, 2017.

Gkikas, K., Proestakis1, E., Amiridis, V., Kazadzis, S., Di Tomaso, E.D., Marinou, E., Hatzianastassiou, N., Kok, J. F., Pérez García-Pando, C.: Quantification of the dust optical depth across spatiotemporal scales with the MIDAS global dataset (2003-2017), Atmos. Chem. Phys., 22, 3553-3578, https://doi.org/10.5194/acp-22-3553-2022, 2022.

Harrison, P., Dunford, A., Barton, D.N., Kelemen, E., Martín-López f, B., Norton, L., Termansen, M., Saarikoski, H., Hendriks, K., Gómez-Baggethun, E., Czúcz, B., García-Llorente, M., Howard, D., Jacobs, S., Karlsen, M., Kopperoinen, L., Madsen, A., Rusch, G., van Eupen, M., Verweij, P., Smith, R., Tuomasjukka, D., Zulian, G.: Selecting methods for ecosystem service assessment: A decision tree approach, Ecosyst. Serv., 29, 481-498, https://doi.org/10.1016/j.ecoser.2017.09.016, 2018.

Hansen, M.C., Potapov, P.V, Hancher, M., Turubanova, S.A., Tyukavina, A., Thau, D., Stehman, S.V.,

https://doi.org/10.5194/essd-2025-107
Preprint. Discussion started: 31 March 2025

Goetz, S.J., Loveland, T.R., kommareddy, A., Georov, A., Chini, L., Justice, C.O., Townshend, J.R.G.: High-Resolution Global Maps of 21st-Century Forest Cover Change, Science., 342(6160), 850-853, https://www.science.org/doi/10.1126/science.1244693, 2013.

Hagen, L.J.: A wind erosion prediction system to meet user needs, J soil water conserv., 46(2), 106-111, 1991.ISSN/ISBN: 0022-4561, 1991.

He, S., Zhu, D., Chen, Y., Liu, X., Chen, Y., Wang, X.: Application and problems of emergy evaluation: A systemic review based on bibliometric and content analysis methods, Ecol. Indic., 114, 106304, https://doi.org/10.1016/j.ecolind.2020.106304, 2020.

Hooper, T., Beaumont, N., Griffiths, C., Langmead, O., Somerfield, P.J.: Assessing the sensitivity of ecosystem services to changing pressures, Ecosyst. Serv., 24, 160-169, https://doi.org/10.1016/j.ecoser.2017.02.016, 2017.

IPBES.: Global assessment report on biodiversity and ecosystem services of the Intergovernmental Science-Policy Platform on Biodiversity and Ecosystem Services, IPBES secretariat, Bonn, Germany, 1148, 1-10, 2019a.

IPBES.: Summary for policymakers of the global assessment report on biodiversity and ecosystem services of the Intergovernmental Science-Policy Platform on Biodiversity and Ecosystem Services, IPBES secretariat, Bonn, Germany, 45, 3, 680-681, 2019b.

Ingwersen W.W.: Uncertainty characterization for emergy values, Ecol. Model., 221, 445-452, https://doi.org/10.1016/j.ecolmodel.2009.10.032, 2010.

Jiang, W., Wu, T., Fu, B.: The value of ecosystem services in China: A systematic review for twenty years, Ecosyst. Serv., 52, 101365, https://doi.org/10.1016/j.ecoser.2021.101365, 2021.

Jiao, W., Wang, L., Smith, W.K., Chang, Q., Wang, H. and D'Odorico, P.: Observed increasing water constraint on vegetation growth over the last three decades, Nat. Commun., 12(1), 3777, https://doi.org/10.1038/s41467-021-24016-9, 2021.

Kuang, W., Zhang, S., Li, X., Lu, D.: A 30 m resolution dataset of China's urban impervious surface area and green space, 2000–2018, Earth Syst. Sci. Data., 13, 63-82, https://doi.org/10.5194/essd-13-63-2021, 2021.

Le Noë, J., Manzoni, S., Abramoff, R., Bölscher, T., Bruni, E., Cardinael, R., Ciais, P., Chenu, C., Clivot, H., Derrien, D., Ferchaud, F., Garnier, P., Goll, D., Lashermes, G., Martin, M., Rasse, D., Rees, F., Sainte-Marie, J., Salmon, E., Schiedung, M., Schimel, J., Wieder, W., Abiven, S., Barré, P., Cécillon, L., Guenet, B.: Soil organic carbon models need independent time-series validation for reliable prediction, Commun Earth Environ., 4, 158, https://doi.org/10.1038/s43247-023-00830-5, 2023.

Li, F., Wang F., Liu, H., Huang, K., Yu,Y., Huang, B.: A comparative analysis of ecosystem service valuation methods: Taking Beijing, China as a case, Ecol. Indic., 154, 110872, https://doi.org/10.1016/j.ecolind.2023.110872, 2023.

Li, C., Gao, Z., Sun, B., Wu, J., Wang, H., Ding, X.: Ecological restoration effects of the Beijing-Tianjin Sandstorm Source Control Project in China since 2000, Ecol. Indic., 146, 109782, https://doi.org/10.1016/j.ecolind.2022.109782, 2023.

Li, B., Xu, X., Liu, X., Shi, Q., Zhuang, H., Cai, Y., He, D.: An improved global land cover mapping in 2015 with 30 m resolution (GLC-2015) based on a multisource product-fusion approach, Earth Syst.

https://doi.org/10.5194/essd-2025-107
Preprint. Discussion started: 31 March 2025

Sci. Data., 15, 2347-2373, https://doi.org/10.5194/essd-15-2347-2023, 2023.

Li, J., He, H., Zeng, Q., Chen, L., Sun, R.: A Chinese soil conservation dataset preventing soil water erosion from 1992 to 2019, Sci Data., 10, 319, https://doi.org/10.1038/s41597-023-02246-4, 2023.

Li, Z., Chen, X., Qi, J., Xu, C., An, J., Chen, J.: Accuracy assessment of land cover products in China from 2000 to 2020, Sci Rep., 13, 12936, https://doi.org/10.1038/s41598-023-39963-0, 2023.

Liu, Y., Zhao, W.W., Zhang, Z.J., Hua, T., Ferreira, C.: The role of nature reserves on conservation effectiveness of ecosystem services in China, J. Environ. Manage., 342, 118228, https://doi.org/10.1016/j.jenvman.2023.118228, 2023.

Liu, Y., Zhao, W.W., Zhang, Z.J., Ding, J.Y., Wang, L.X.: A high spatial resolution dataset of ecosystem services of 2000-2020 in China[data set], https://doi.org/10.57760/sciencedb.20797, 2025.

Liu X, Zhao, W, Yao, Y, Pereira, P.: The rising human footprint in the Tibetan Pateau threatens the effectiveness of ecological restoration on vegetation growth, J. Environ. Manage., 351, 119963, https://doi.org/10.1016/j.jenvman.2023.119963, 2024.

Liy, B.Y., Nearing, M.A., Risse, L.M.: Slope gradient effects on soil loss for steep slopes, Transactions of the ASAE., 37(6), 1835-1840, https://www.researchgate.net/publication/2706137061994, 1994..

Lu, F., Hu, H., Sun, W., Yu, G.: Effects of national ecological restoration projects on carbon sequestration in China from 2001 to 2010, Proc. Natl Acad. Sci. USA., 115, 4039-4044, https://doi.org/10.1073/pnas.1700294115, 2018.

Markham, B.L., Helder, D.L.: Forty-year calibrated record of earth-reflected radiance from Landsat: a review, Remote Sens. Environ., 122, 30-40, https://doi.org/10.1016/j.rse.2011.06.026, 2012.

Mccool, D.K., Brown, L.C., Foster, G.R., Mutchler, C.K., Meyer, L.D.: Revised slope steepness factor for the Universal Soil Loss Equation, Transactions of the ASAE., 30(5), 1387-1396, https://doi.org/10.13031/2013.30576, 1987.

Meng, N., Yang, Y., Zheng, H., Li, R.: Climate change indirectly enhances sandstorm prevention services by altering ecosystem patterns on the Qinghai-Tibet Plateau, J Mt Sci., 1711-1724, https://doi.org/10.1007/s11629-020-6526-0, 2021.

Millennium Ecosystem Assessment: Ecosystems and Human Well-Being: Synthesis, Washington, DC: Island Press, 2005.

Monte-Luna, P.D., Brook, B.W., Zetina-Rejón, M.J., Cruz-Escalona, V.H.: The carrying capacity of ecosystems, Glob. Ecol. Biogeogr., 13(6), 485-495, https://doi.org/10.1111/j.1466-822X.2004.00131.x, 2004.

Mugiraneza, T., Ban, Y., Haas, J.: Urban land cover dynamics and their impact on ecosystem services in Kigali, Rwanda using multi-temporal Landsat data, RSASE., 13, 234-246, https://doi.org/10.1016/j.rsase.2018.11.001, 2019.

Ouyang, Z., Song, C., Zheng, H., Polasky, S., Xiao, Y., Bateman, I., Liu, J., Ruckelshaus, M., Shi, F., Xiao, Y., Xu, W., Zou, Z., Daily, G.C.: Using gross ecosystem product (GEP) to value nature in decision making, Proc. Natl. Acad. Sci., 117 (25), 14593-14601, https://doi.org/10.1073/pnas.1911439117, 2020.

Ouyang, Z., Zheng, H., Xiao, Y., Polasky, S., Liu, J., Xu, W., Wang, Q., Zhang, L., Xiao, Y., Rao, E., Jiang, N., Lu, F., Wang, X., Yang, G., Gong, S., Wu, B., Zeng, Y., Yang, W., Daily, G.C.: Improvements

https://doi.org/10.5194/essd-2025-107
Preprint. Discussion started: 31 March 2025

in ecosystem services from investments in natural capital, Sci. Adv., 2(2), e1500961, https://doi.org/10.1126/science.aaf2295, 2016.

Pandeya, B., Buytaert, W., Zulkafli, Z., Karpouzoglou, T., Mao, F., Hannah, D.M.: A comparative analysis of ecosystem services valuation approaches for application at the local scale and in data scarce regions, Ecosyst. Serv., 250-259, https://doi.org/10.1016/j.ecoser.2016.10.015, 2016.

Peng, Y., Chen, W., Pan, S., Gu, T., Zeng, J.: Identifying the driving forces of global ecosystem services balance, 2000-2020, J. Clean. Prod., 426, 13901, https://doi.org/10.1016/j.jclepro.2023.139019, 2023.

Piao, S., Wang, X., Park, T., Chen, C., Lian, X., He, Y., Bjerke, J., Chen, A., Ciais, P., Tømmervik, H., Nemani, R., Myneni, B.: Characteristics, drivers and feedbacks of global greening, Nat. Rev. Earth Envir., 1, 14-27, https://doi.org/10.1038/s43017-019-0001-x, 2020.

Rao, W., Shen, Z., Duan, X.: Spatiotemporal patterns and drivers of soil erosion in Yunnan, Southwest China: RULSE assessments for recent 30 years and future predictions based on CMIP6, Catena., 220, 106703, https://doi.org/10.1016/j.catena.2022.106703, 2023.

Richardson, A.D., Hollinger, D.Y., Burba, G.G., Davis, K.J., Flanagan, L.B., Katul, G.G., Munger, J.W., Ricciuto, D.M., Stoy, P C., Suyker, A.E., Verma, S.B., Wofsy, S.C.: A multi-site analysis of random error in tower-based measurements of carbon and energy fluxes, Agr. Forest. Meteorol., 136, 1-18, https://doi.org/10.1016/j.agrformet.2006.01.007, 2006.

Spawn, S.A., Gibbs, H.K.: Global aboveground and belowground biomass carbon density maps for the year 2010 [data set], https://doi.org/10.3334/ORNLDAAC/1763, 2020.

Song, Z., Yang, H., Huang, X., Ma, M.: The spatiotemporal pattern and influencing factors of land surface temperature change in China from 2003 to 2019, Int J Appl Earth Obs Geoinf., 104, 102537, https://doi.org/10.1016/j.jag.2021.102537, 2021.

Walther, F., Barton, D., Schwaab, J., Kato-Huerta, J., Immerzeel, B., Adamescu, M., Andersen, E., Coyote, M., Arany., I, Balzan, M., Bruggeman, A., Carvalho-Santos, C., Cazacu, C., Geneletti, D., Giuca, R., Inácio, M., Lagabrielle, E., Lange, S., Le Clec'h, S., Vanessa Lim, Z., Mörtberg, U., Nedkov, S., Portela, A., Porucznik, A., Racoviceanu, T., Rendón, P., Ribeiro, D., Seguin, J., Hribar, M., Stoycheva, V., Vejre, H., Zoumides, C., Grêt-Regamey, A.: Uncertainties in ecosystem services assessments and their implications for decision support – A semi-systematic literature review, Ecosyst. Serv., 73, 101714, https://doi.org/10.1016/j.ecoser.2025.101714, 2025.

Wan, Z.: New refinements and validation of the collection-6 MODIS land-surface temperature/emissivity product, Remote Sens. Environ., 140, 36-45, https://doi.org/10.1016/j.rse.2006.06.026, 2014.

Wang, S., Fu, B., Piao, S., Lu, Y., Ciais., Feng, X., Wang, Y: Reduced sediment transport in the Yellow River due to anthropogenic changes, Nat. Geosci., 9, 38-41, https://doi.org/10.1038/ngeo2602, 2016.

Wang, L., Jiao, W., MacBean, N., Rulli, M.C., Manzoni, S., Vico, G., D ' Odorico, P.: Dryland productivity under a changing climate, Nat. Clim. Chang., 12, 981-994, https://doi.org/10.1038/s41558-022-01499-y, 2022.

Wang, H., Zhan, J., Wang, C., Chen, B., Yang, Z., Bai, C.: Short-term fluctuations of ecosystem services beneath long-term trends, Resour. Conserv. Recy., 203, 107454, https://doi.org/10.1016/j.resconrec.2024.107454, 2024.

https://doi.org/10.5194/essd-2025-107
Preprint. Discussion started: 31 March 2025

Williams, J.R., Jones, C.A., Dyke, P.T.: A modeling approach to determining the relationship between erosion and soil productivity, Transactions of the ASAE., 27(1): 129-144, https://doi.org/10.13031/2013.32748, 1984.

Wischmeier, W.H., Smith, D.D.: Predicting Rainfall Erosion Losses - A Guide to Conservation Planning, U.S. Department of Agriculture, Washington, D.C, Agriculture Handbook No. 537, 1978.

Wu, Q., Yang, L., Mi, J.: Detecting the effects of opencast mining on ecosystem services value in arid and semi-arid areas based on time-series remote sensing images and Google Earth Engine (GEE). BMC, Ecol. Evo., 24, 28, https://doi.org/10.1186/s12862-024-02213-6, 2024.

Xiao, Q., Hu, D., Xiao, Y.: Assessing changes in soil conservation ecosystem services and causal factors in the Three Gorges Reservoir region of China, J. Clean Prod., 163, S172-S180, https://doi.org/10.1016/j.jclepro.2016.09.012, 2017.

Xu, W., Xiao, Y., Zhang, J., Yang, W., Zhang, L., Zheng, H., Liu, J., Polasky, S., Jiang, L., Xiao, Y., Shi, X., Rao, E., Lu, F., Wang, X., Daily, G.C., Ouyang, Z.: Strengthening protected areas for biodiversity and ecosystem services in China, Proc. Natl. Acad. Sci. U.S.A., 114(7), 1601-1606, https://doi.org/10.1073/pnas.1620503114, 2017.

Yang, Y., Roderick, M.L., Guo, H., Miralles, D., Zhang, L., Fatichi, S., Luo, Y., Zhang, Y., McVicar, T., Tu, Z., Keenan, T., Fisher, J., Gan, R., Zhang, X., Piao, S., Zhang, B., Yang, D.: Evapotranspiration on a greening Earth, Nat Rev Earth Environ., 4, 626-641, https://doi.org/10.1038/s43017-023-00464-3, 2023.

Yang, Y., Xiao, P., Feng, X. Li, H.: Accuracy assessment of seven global land cover datasets over China, ISPRS J. Photogramm. Remote. Sens., 125, 156-173, https://doi.org/10.1016/j.isprsjprs.2017.01.016, 2017.

Yin, L., Wang, W., Wang, Y.: National Ecological Barrier Zone 1-km Resolution Water Production Dataset (2000-2015) [data set], Journal of Global Change Data & Discovery, 4(4), 332-337, https://doi.org/10.3974/geodp.2020.04.03, 2020.

Zhao, M., Zhang, J., Velicogna, L., Liang, C., Li, Z.: Ecological restoration impact on total terrestrial water storage, Nat Sustain., 4, 56-62, https://doi.org/10.1038/s41893-020-00600-7, 2021.

Zhao, B., Mao, K., Cai, Y., Shi, J., Li, Z., Qin, Z., Meng, X., Shen, X., Guo, Z.: A combined Terra and Aqua MODIS land surface temperature and meteorological station data product for China from 2003-2017, Earth Syst. Sci. Data., 12 (4), 2555-2577, https://doi.org/10.5194/essd-12-2555-2020, 2020.

Zhao, M., Running, S.W.: Drought-induced reduction in global terrestrial net primary production from 2000 through 2009, Science., 329(5994), 940-943, https://doi.org/10.1126/science.1192666, 2010.

Zhang, Z., Zhao, W., Liu, Y., Pereira, P.: Impacts of urbanisation on vegetation dynamics in Chinese cities, Environ. Impact Assess. Rev., 103, 107227, https://doi.org/10.1016/j.eiar.2023.107227, 2023.

Zhu, W.Q.: Estimation of net primary productivity of Chinese terrestrial vegetation based on remote sensing and its relationship with global climate change, Ph.D. thesis, Beijing Normal University., Beijing, 2005.

Zobeck, T.M., Parker N.C., Haskell, S., Guoding, K.: Scaling up from field to region for wind erosion prediction using a field-scale wind erosion model and GIS, Agric ecosyst environ., 82(1), 247-259,

https://doi.org/10.5194/essd-2025-107
Preprint. Discussion started: 31 March 2025

Open Access Earth System Science Data Discussions

https://doi.org/10.1016/S0167-8809(00)00229-2, 2000.